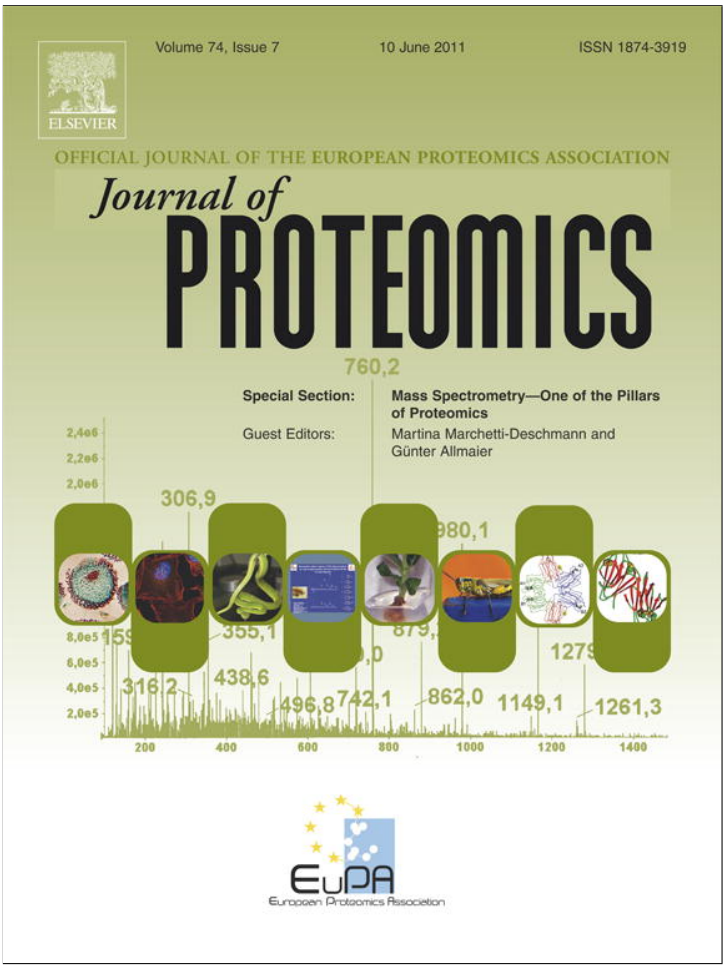

JOURNAL OF PROTEOMICS 74 (2011) 993–1001

available at www.sciencedirect.com

ScienceDirect

www.elsevier.com/locate/jprot

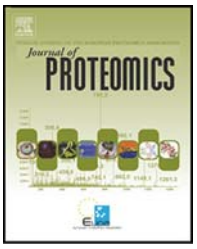

Protein identification with Liquid Chromatography and Matrix Enhanced Secondary Ion Mass Spectrometry (LC-ME-SIMS)

Luke MacAleese[a], *Marc C. Duursma*[a], *Leendert A. Klerk*[a], *Greg Fisher*[b], *Ron M.A. Heeren*[a,c,*]

[a]*FOM-Institute for Atomic and Molecular Physics, Science Park 104, 1098 XG Amsterdam, The Netherlands*
[b]*Physical Electronics, 18725 Lake Drive East, Chanhassen, MN 55317, USA*
[c]*Netherlands Proteomics Centre, Padualaan 8, 3584 CH Utrecht, The Netherlands*

ARTICLE INFO

Article history:
Received 30 September 2010
Accepted 9 February 2011
Available online 17 February 2011

Keywords:
ME-SIMS
Peptide mass fingerprinting
Imaging MS
Proteins

ABSTRACT

Secondary Ion Mass Spectrometry (SIMS) is a well established method for sensitive surface atomic and molecular analysis. Protein analysis with conventional SIMS has been attempted numerous times; however it delivers exclusively fragment peaks assigned to α-amino acids or immonium ions. In this paper we report experiments where direct sequence information could be measured thanks to a combination of HPLC separation with matrix enhanced SIMS (ME-SIMS) on tryptic digests of intact proteins. We employ peptide mass fingerprinting (PMF) and protein identification through the detection of HPLC-separated digests of Savinase (Sav.) and bovine serum albumin (BSA), followed by MASCOT search. This is the first time that the possibility of full protein identification using LC-ME-SIMS is demonstrated in a classic proteomics workflow and that a 69 kDa protein is identified with SIMS. These results demonstrate both the relevance and the potential of LC-ME-SIMS in future high resolution proteomics studies.

1. Introduction

Secondary Ion Mass Spectrometry (SIMS) is a well established method for sensitive surface analysis [1]. It has numerous successful applications in the semiconductor industry, polymer science, paint analysis and the life sciences. Static SIMS, defined by the usage of a primary ion dose below 10^{13} ions/cm^2 has two distinctive advantages over other MS based surface analysis techniques: 1) Less than 1% of the surface area is probed to a depth of approximately 5 nm of the surface. This ensures exquisite surface sensitivity with very little material removal. 2) High spatial resolution can be obtained with commercially available instruments reaching sub-50 nm "lateral resolution".

In the field of mass spectrometric imaging (MSI) [2,3], the characteristics of SIMS have long been appreciated and the literature shows a steady increase in the number of publications in surface analysis of biologically relevant samples such as tissues, tissue sections, biopolymers and bacterial cultures [4–9]. Biological imaging MS with SIMS is particularly relevant considering the possibility to image beyond the cellular scale [10]. However, sensitivity and speed of analysis are considered drawbacks of the technique, especially in the new directions in SIMS based MSI, with a large emphasis towards gaining proteomics information [11].

Several strategies have been explored recently to use SIMS for protein identification. Desorption and ionization methodologies have been developed that reduce surface fragmentation through the use of larger primary ion species such as molecular cluster ions or molecular ions [12]. These instrumental developments have led to enhanced ionization of intact surface molecules, resulting in considerable effective sensitivity gain in a mass range up to a few kDa. The use of such primary ion source extends the practical molecular weight range amenable for SIMS analysis. Another equally

* *Corresponding author at:* FOM-AMOLF, Science Park 104, 1098 XG Amsterdam, The Netherlands. Tel.: +31 20 7547100.
E-mail address: heeren@amolf.nl (R.M.A. Heeren).

1874-3919/$ – see front matter © 2011 Elsevier B.V. All rights reserved.
doi:10.1016/j.jprot.2011.02.009

important development to improve the analysis of intact biomolecules is Matrix Enhanced-SIMS (ME-SIMS) [13]: a sample preparation methodology for SIMS that takes advantage of developments in matrix assisted laser desorption and ionization (MALDI). In ME-SIMS the surface to be analyzed is covered with a protonating matrix prior to analysis. The matrices employed are the typical MALDI matrices, 2,5-dihydroxybenzoic acid (DHB), alpha-cyano-cinnamic acid (HCCA) and the like. It was shown that the tissue extraction properties of this sample preparation step remained the same as for MALDI, although the UV absorption properties of the matrix were not required to produce pseudo-molecular ions with ME-SIMS. It was shown that identical spectra could be obtained up to several kDa in ME-SIMS and MALDI for a variety of compound classes [11]. The combination of cluster/molecular ion beams with ME-SIMS has been demonstrated [14] to cumulatively enhance sensitivity for intact molecule analysis with MSI at high spatial resolution and provide mass spectral information that localizes and identifies small molecules, lipids and peptides directly on tissue surfaces.

Protein analysis with conventional SIMS has been attempted numerous times. It was shown that SIMS analysis of proteins delivers exclusively fragment peaks that are assigned to α-amino acids or immonium ions. In a mixture of 14 known proteins it was demonstrated to be possible to semi-quantitatively distinguish the individual proteins using Principal Component Analysis based on the fragment fingerprints [15]. However, no direct sequence information could be obtained in these studies. Recent studies use intrinsic peptide fragmentation with cluster beams to employ larger fragments of isolated standards for direct peptide analysis (without a matrix addition) working towards the application of cluster SIMS in proteomics [16].

In this paper, we set out to extend the capabilities of ME-SIMS through the addition of a liquid chromatography separation step in our analytical workflow. This for the first time demonstrates the possibility of full protein identification using LC-ME-SIMS in proteomics. We employ peptide mass fingerprinting (PMF) and protein identification through the detection of the LC-separated digests of Savinase (Sav.) and bovine serum albumin (BSA), followed by MASCOT search.

2. Materials and methods

2.1. Sample preparation

Savinase (subtilisin Savinase/*Bacillus lentus* alkaline serine protease containing 269 amino acids, 26,689 Da) and BSA (serum albumin/*Bos taurus* plasma protein containing 607 amino acids, 69,293 Da) proteins were obtained from Sigma-Aldrich, Zwijndrecht, The Netherlands. Trypsin (*Sus scrofa*) was obtained from Promega Benelux B.V. Leiden, The Netherlands. Solvents (water and acetonitrile), buffers and saline (PBS and Tris–HCl) were obtained from Sigma-Aldrich. Aqueous solutions of proteins were prepared just before use with similar concentration for both proteins, around 100 μM. 200 μL of those solutions was mixed with trypsin in Tris–HCl solution in a molar ratio of 1:50 trypsin:protein. Digestion was performed at 37 °C overnight. BSA was digested with trypsin only, whereas for Savinase a combined CNBr and trypsin digestion was used. After digestion, peptide solutions were cleaned and separated by nanoLC. The nanoLC-system (LCPackings, Amsterdam, the Netherlands) consists of an autosampler, a switching unit, a nanoflow system and UV detector. The switching unit is equipped with a reverse-phase capillary precolumn (C18 PepMap 100, internal diameter 0.3 mm, length 1 mm) and is used for preconcentration of the sample at a flowrate of 30 μL/min. Peptide separation is then carried out on an analytical column (PepMap 100, internal diameter 0.075 mm, length 15 cm) using nanoflow elution at 300 nL/min. Typically, the injection volume was 2 μL. The eluents used were 1% acetic acid and 5% acetonitrile in water (A) and 1% acetic acid and 5% water in acetonitrile (B), with a gradient of 0–30 min: 0–50% B, followed by 30–35 min: 50–90% B.

The output capillary of the nanoLC-system was connected to an AB-SymBiot® workstation. Using this automated device, 100 LC-fractions were deposited every 30 s on a target plate. The fractions were collected during 50 min, including the entire elution pattern of the digested peptides (see UV trace in Fig. 1). Fractions were deposited in a 10-by-10 spot array with a pitch of 1 mm between fractions in all directions, resulting in a total pattern of 1 cm^2 as schematically shown in Fig. 1. Fractions were deposited on a pre-coated 2,5-DHB-foil (TIME MALDI-MS Foil, LabConnections).

2.2. Mass spectrometry

Secondary Ion Mass Spectrometry (SIMS) was performed on two Physical Electronics (PHI) instruments.

A TRIFT-II is equipped with a gold liquid metal ion gun (LMIG). 22 keV Au^+ primary ions were microfocused on the sample surface. The primary ion current was 0.4 nA. The total primary ion dose density amounted to $1.15 \cdot 10^{10}$ ions/cm^2, which is well below the static limit. Positive secondary ions were extracted to the mass analyzer with a static voltage of 3.5 kV, and post accelerated in front of the detector (dual stage MCP) by an additional 10 kV. In order to optimize sensitivity at high mass-to-charge (*m/z*), only ions in the mass range 500–3500 *m/z* were allowed to reach the detector. The full LC pattern was imaged step-by-step in a mosaic formed by 128×128 individual tiles between which the stage moved. Each tile of about 90 μm wide was probed by the primary ion beam in a 256×256 raster for 3 s. The resulting image was saved as a RAW file.

A second C_{60} TOF-SIMS experiment was performed using a Physical Electronics (Chanhassen, MN) TRIFT V nanoTOF that is equipped with a 20 kV C_{60} primary ion gun. The C_{60} column is oriented at 48° from surface normal and was operated such that the sample was interrogated by a mass pure C_{60}^+ analytical ion beam. The DC current of the C_{60}^+ primary ion beam was 0.36 nA, and the analytical field-of-view (FOV) was 400 μm×400 μm. A primary ion dose density (PIDD) of 5.2×10^{10} C_{60}^+/cm^2, digitally rastered over 256×256 pixels, was delivered to the sample during the 3 minute analysis of each elution spot. Data in the positive secondary ion polarity (+SIMS) was collected in the *m/z* range of 0–5000 *m/z* and saved into a raw data stream file for off-line retrospective data analysis and data mining. A post-acceleration voltage of 15 kV was used to increase the conversion efficiency (i.e. sensitivity) of the dual microchannel plate (DMCP) detector at high *m/z* ratios for peptide mass fingerprinting.

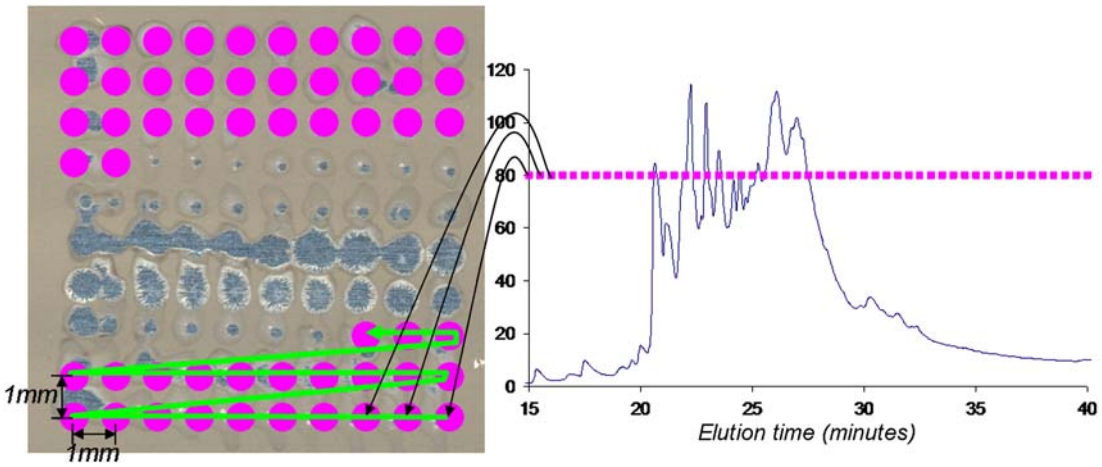

Fig. 1 – Scheme of the nanoLC fraction deposition on the 2,5-DHB-coated plate. 15 min after injection fractions start to be deposited in a 10-by-10 array using a fly-back pattern. After 20 min, peptides start to be eluted from the column, as can be seen from the UV trace on the right.

2.3. *Data analysis*

The TRIFT associated software WinCadence (v4.4 Physical Electronics, Chanhassan, USA) was used to perform manual peak picking on each spectrum file resulting from the nanoTOF profiling experiments.

RAW images were converted to datacubes [3] with the MSTools software suite developed at AMOLF. The datacube format enables direct observation of mass selected images while browsing through *m/z* values, and fast region-of-interest (ROI) selection together with spectral comparison between ROIs and the global image. For imaging datasets, manual peak picking was performed by selecting each droplet as a ROI and observing its specific peaks with regard to the total image spectrum.

3. Results and discussion

3.1. *Efficient peptide detection with SIMS after LC*

Trypsin digestion of Savinase and bovine serum albumin produces peptides that can be separated by liquid chromatography as illustrated in Fig. 1. Fig. 2-A shows the disposition of LC fractions in a ten-by-ten pattern where each position is tagged with an elution time. The whole pattern is imaged by SIMS as can be seen in the total ion current (TIC) image. Fig. 2-B and the contour of each fraction is clearly recognized from the different ionization properties of the LC droplets versus the ionization of the intact matrix coating. More interestingly, Fig. 2-C to F displays the mass selected images of the full LC trace of Savinase digest, where selected peaks are assigned to four different peptide sequences expected from Savinase digestion. Fig. 2-C to F represents the different fraction localizations of respectively sequence QKNPSWSNVQIR (fragment 230–241 with *m/z* 1456.4), AQSVPWGISR (fragment 1–10 with *m/z* 1100.2), GVLVVAASGNSGAGSISYPAR (fragment 144–164 with *m/z* 1932.4) and NTATSLGSTNLYGSGLVNAEAATR (fragment 246–269 with *m/z* 2368.0). It is interesting to note that despite their high molecular weight relative to usual SIMS detection mass range, peptides are properly observed on mass spectra (mass spectra are available as supplementary data). The high detection efficiency is illustrated in Fig. 3, displaying the mass spectra of HPLC fraction numbers 29 and 44 of the Savinase digest, measured in the C_{60} profiling experiment. Peaks up to nearly 5 kDa are detected with high S/N and can again be assigned to digested sequences such as *m/z* 4591 in fraction 29 corresponding to fragment sequence 45–92 (GGASFVP-GEPSTQDGNGHGT HVAGTIAALNNSIGVLGVAP SAELYAVK) and *m/z* 3612 in fraction 44 corresponding to fragment sequence 181–216 (ASFSQYGAGLDIVAPGVNVQ STYPGSTYASLNGTSM). This high detection efficiency can be related to two instrumental parameters. Firstly, the use of a C_{60} primary ion gun induces less fragmentation compared to the use of atomic primary ions, which is the reason why we can detect intact digested peptides. C_{60} primary ions additionally provide high sputtering and ionization efficiency that increase sensitivity on the whole mass range. Secondly, the use of high post acceleration voltages counteracts the loss of sensitivity of MCP detectors for ions with high *m/z*. The use of a liquid separation technique further improves the detection efficiency as it substantially reduces the complexity of the analyte which in turn results in a reduction of ion suppression effects. In each LC fractions only a small number of digested peptides remain of which the relative concentration increases dramatically versus direct analysis of digestion mixture. This characteristic is particularly important when considering SIMS which is particularly sensitive to ion suppression effects and where all charges are prone to be captured by compounds which ionize best. Thus, the combination of a LC separation step before SIMS analysis reveals to be particularly fruitful for detection efficiency towards large *m/z*.

3.2. *Separation and relevant peak picking*

It is remarkable that on mass-selected images (Fig. 2-C to F), peptides appear only at well-defined positions corresponding to the specific LC fraction where they are eluted. This constitutes

JOURNAL OF PROTEOMICS 74 (2011) 993–1001

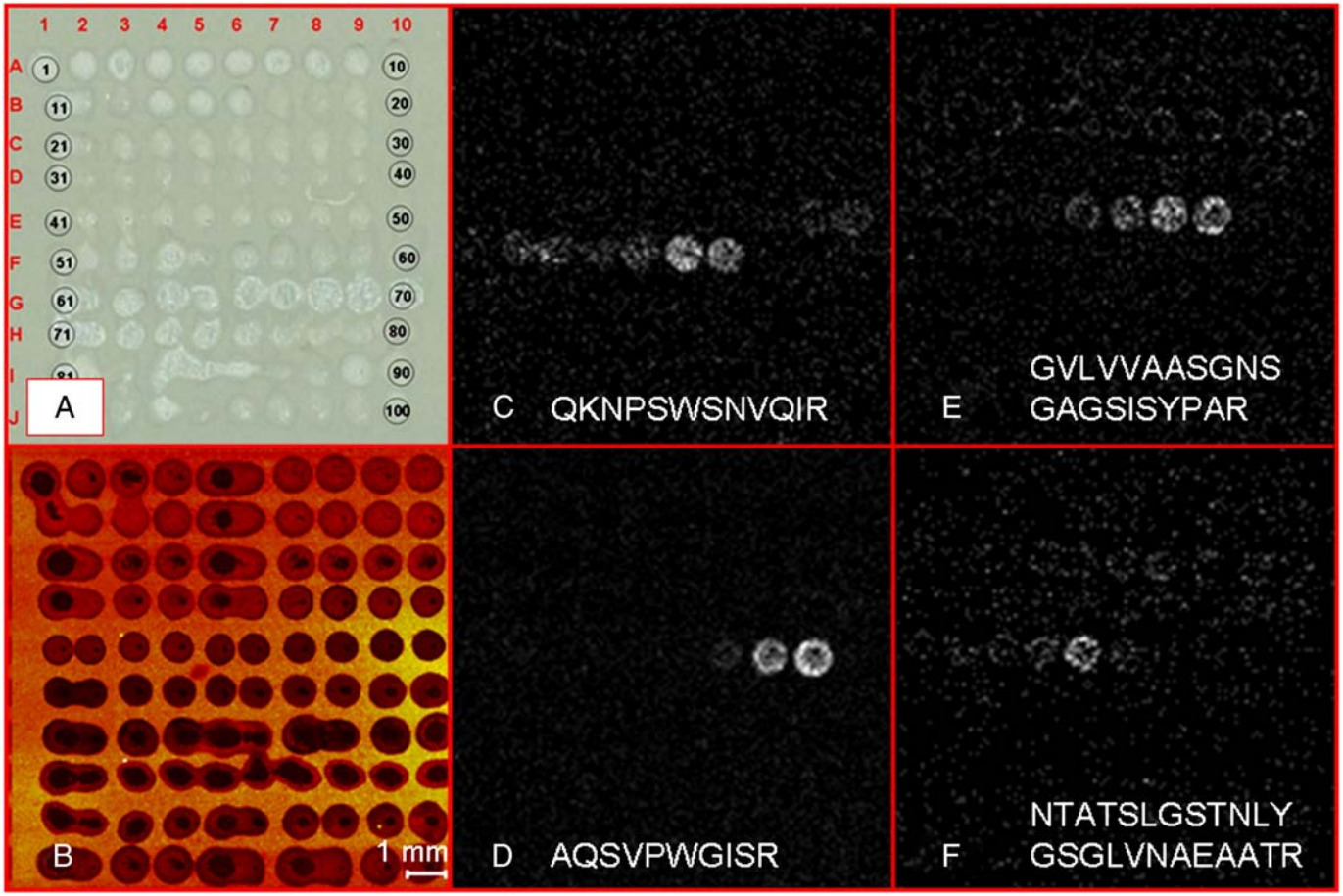

Fig. 2 – (A) Optical image of a liquid chromatography trace separated in 100 fractions of 30 s deposited at 1 mm interval in a 10 × 10 matrix. (B–F) SIMS images of a similar LC trace: (B) total ion current (TIC) image, followed by mass selected images of 4 peaks assigned to peptides from Savinase trypsin digest. (C) Sequence 230–241: QKNPSWSNVQIR (*m/z* 1456.4); (D) sequence 1–10: AQSVPWGISR (*m/z* 1100.2); (E) sequence 144–164: GVLVVAASGNSGAGSISYPAR (*m/z* 1932.4); (F) sequence 246–269: NTATSLGSTNLYGSGLVNAEAATR (*m/z* 2368.0). Peptides are well separated by liquid chromatography and appear in different fractions corresponding to different elution times. (Respective mass spectra are provided in supplementary data).

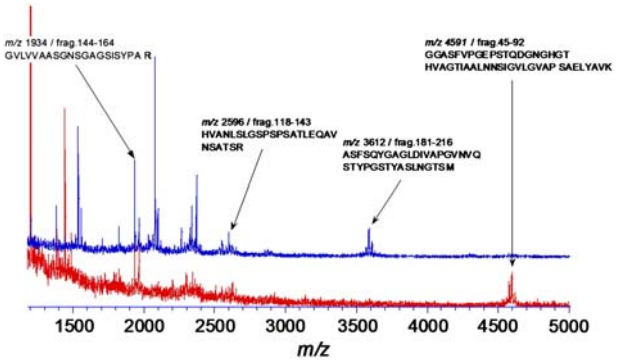

Fig. 3 – Mass spectra of fractions #29 (bottom) and #44 (top). Peptide sequences are detected up to 5 kDa.

an important element to discriminate real digested peptides that appear in a limited number – one to three – of LC fractions from chemical noise or contaminants that lack specific localization. Since each fraction has a time-tag, it is also possible to reconstruct time resolved mass spectra (Fig. 4) after profiling or imaging the whole LC trace. This 2-dimensional representation provides an equivalent view of the separation result as given by the spatial imaging of the LC trace. Spatial resolution in imaging MS gives insight on the LC time separation, and both space and time separations can be used to discriminate relevant peaks in mass spectra. Relevant peak picking can therefore be done either on "spatial-image" or on "temporal-image". In either case, the relevance criterion is met when peaks are present in only a limited number of adjacent fractions. A peak list can be established by browsing imaging datasets along the *m/z* axis. This investigation type requires no data-processing and is thus very simple and can be done manually.

Alternatively non-supervised statistical analysis tools can beused such as Principal Component Analysis (PCA) as implemented in ChemomeTricks [17]. This program toolbox is used for multiple data preparation steps such as conversion from raw files, spatial and spectral binning, baseline subtraction and peak picking, as well as for statistical analysis. The first principal component resulting from PCA, i.e. the component describing the highest variance in the dataset, separates LC droplets from the matrix-coated target plate (Fig. 5). The high variance in this direction reflects the fact that there are more spectral differences between the ensemble of the LC fractions and the rest of the matrix target than within the LC-fractions or the matrix spectra. The matrix spectra are so homogeneous and reproducible that the variance between them is very small, which explains why they constitute the first principal component direction. This spatial discrimination between LC droplets and the DHB-target plate can be used with two purposes: exclusively extract peptide mass spectra from the LC fractions, while at the same time removing contaminant and matrix peaks from the dataset prior to further analysis. This procedure is referred to as PCA-guided selection of an analytical region-of-interest. All mass spectra that belong to pixels that have a high negative score on the first principal component are discarded from the dataset. This approach results in a reduced dataset that exclusively contains spectra measured inside droplets. Subsequently, all mass features presenting high loadings outside the droplets are removed from the dataset. An empirical minimal threshold is considered for the absolute loading value of features to be removed so that only peaks that are strongly characteristic of the matrix-coated target are removed. This threshold avoids accidental removal of features that do not significantly participate in the global separation of inside/outside LC droplets. Those peaks could indeed still be responsible for inter-droplet variance and therefore be assigned to actual digested peptide peaks. The two steps contribute to significant spectral cleaning and data reduction.

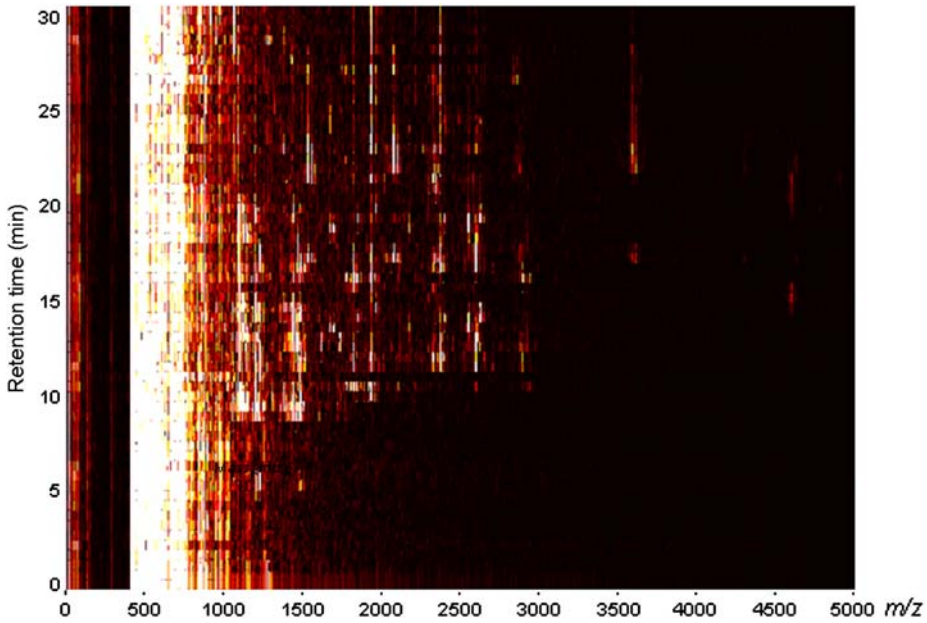

Fig. 4 – Reconstructed LC trace displaying full mass spectra in a time resolved manner. Peaks corresponding to digested peptides especially above 1000 *m/z* and up to 5000 *m/z* show up only when they are eluted from the LC column.

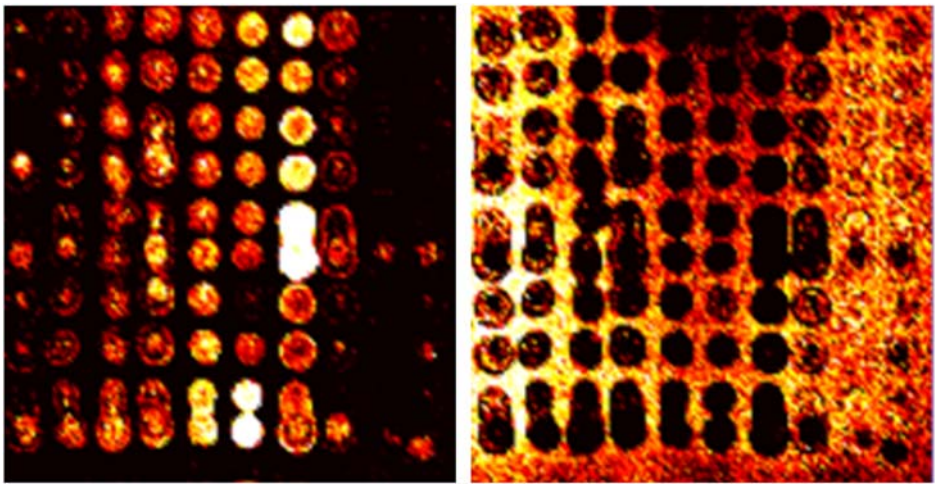

Fig. 5 – Positive (left) and negative (right) scores of image mass spectra projected on the first principal component.

Both investigations – performed manually or through PCA – are conclusive and lead to assignment of numerous predicted digested peptides (see Tables 1 and 2 for list of peptides detected for two proteins, respectively Savinase and bovine serum albumin).

Tables 1 and 2 list the peptide sequences resulting from theoretical *in silico* digestion (allowing 1 miscleavage) of respectively Savinase and bovine serum albumin. Trypsin autolytic peptides are also indicated when observed. Calculated mono-isotopic masses of peptides are considered in association with protonation and adduct formation with sodium and potassium. It is remarkable that about 50% (12/24) of Savinase digested peptides above 1000 Da are detected. This is the first time intact peptides of such length/weight have been detected with SIMS and a proteomics experiment performed with SIMS as mass spectrometry tool for protein identification. This list in Table 1 is established by close examination of the SIMS spectra targeting peptide peaks at expected *m/z*, and the result demonstrates the potential of using SIMS in a proteomics workflow.

3.3. *MASCOT search*

Above we have shown that the selected peaks corresponded closely to those expected from theoretical *in silico* digestion. In this section we emphasize the compatibility of LC-ME-SIMS with proteomics through the application of a database search for protein identification. For this purpose we use a standard MASCOT PMF database search. We consider the experimental peak lists associated with $[M+H]^+$ – as observed directly and reconstructed from observed cluster *m/z* – from Tables 1 and 2. Each list is used as entry in a Mascot search of the MSDB database. Entry parameters reflect the respective digestion protocols used: trypsin or CNBr/trypsin, allows 1 missed cleavage and utilizes a peptide mass tolerance of 1 Da, wide enough to compensate for suboptimal calibration of the SIMS instrument for this unusually large mass range. The results, as shown in Table 3, unambiguously lead to the identification by peptide mass fingerprinting of both proteins: Savinase, 26 kDa, and BSA, 69 kDa. Savinase is identified with a score 128 and 10 matches representing a sequence coverage of 46%,

Table 1 – Experimentally observed peptides from Savinase tryptic digest. Experimental as well as associated theoretical masses are presented together with the position of the HPLC fraction where observed. Fractions are numbered in the form [#column and #row] where #column and #row range from 1 to 10, which corresponds to the fraction position in the droplet pattern on 2,5-DHB substrate. Deposition starts at [1;1]. The tentatively assigned peptide sequences are characterized by their position in the protein and the number of miscleavages.

Exp. observed *m/z*	Fraction	$[M-H_2O+H]^+$	$[M+H]^+$	$[M+Na]^+$	$[M+K]^+$	Position	#MC		Peptide sequence
1100.2; 1122.4	[7–9;6]; [8–9;6]		1100.58	1122.57		1–10	0	sav	AQSVPWGISR
1154	[2;6]		1154.51			158–168	0	tryp	SSYPGQITGNM
1160.2	[1–2;6]		1159.55			170–180	0	sav	AVGATDQNNNR
1200.4	[9–10;6]		1200.61			232–241	0	sav	NPSWSNVQIR
1204.3; 1228.2	[9–10;6]; [4;6]		1205.70	1227.68		217–229	0	sav	ATPHVAGAAALVK
1439.4; 1456.4	[9–10;6]; [6–7;5]	1438.76	1456.77			230–241	1	sav	QKNPSWSNVQIR
1444; 1460.8; 1484.6; 1499.3	[6–7;5]; [9–10;6]; [4–5;6]	1443.84	1461.85	1483.84	1499.81	217–231	1	sav	ATPHVAGAAALVKQK
1685.8	[5;7]		1662.90	1684.89		11–27	1	sav	VQAPAAHNRGLTGSGVK
1769.8	[4;8]		1768.80			116–133	0	tryp	SCAAAGTECLISGWGNTK
1820.6	[6–7;6]		1820.99			28–44	0	sav	VAVLDTGISTHPDLNIR
1932.4	[6–8;6]		1933.01			144–164	0	sav	GVLVVAASGNSGAGSISYPA R
2368	[5;6]		2368.17			246–269	0	sav	NTATSLGSTNLYGSGLVNAE AATR

Table 2 – Experimentally observed peptides from bovine serum albumin (and trypsin) digest. Experimental as well as associated theoretical masses are presented together with the position of the HPLC fraction where observed. Fractions are numbered in the form [#column and #row] where #column and #row range from 1 to 10, which corresponds to the fraction position in the droplet pattern on 2,5-DHB substrate. Deposition starts at [1;1]. The tentatively assigned peptide sequences are characterized by their position in the protein and the number of miscleavages.

Exp. observed m/z	Fraction	$[M-H_2O+H]^+$	$[M+H]^+$	$[M+Na]^+$	$[M+K]^+$	Position	#MC		Peptide sequence
1012.47	[8;4]; [8+9+10;3]		974.45		1012.41	37–44	0	bsa	DLGEEHFK
1025.26	[7;5]; [9+10;4]		987.53		1025.49	29–36	1	bsa	SEIAHRFK
1025.26	[7;5]; [9+10;4]		987.56		1025.53	212–220	1	bsa	VLASSARQR
1003.45; 1025.26	[7;5]; [9+10;4]; [7+8;5]		1002.58	1024.57		598–607	0	bsa	LVVSTQTALA
1006.45	[1;3]		1006.49			148–157	0	tryp	APVLSDSSCK
1012.47; 1034.35	[8;4]; [4+5;3]; [8+9+10;3]		1011.42	1033.4		413–420	0	bsa	QNCDQFEK
1036.25	[1;3]		1014.6	1036.6		549–557	0	bsa	QTALVELLK
997.45	[7;5]	997.5272	1015.5			310–318	0	bsa	SHCIAEVEK
1006.45; 1025.26; 1047.37; 1063.11	[1;3]; [7;5]; [9+10;4]; [8;4]	1006.4945	1024.46	1046.44	1062.41	499–507	0	bsa	CCTESLVNR
1034.35; 1090.86; 1074.07	[4+5;3]; [8;4]; [8+9+10;3]	1034.4894	1052.4	1074.43	1090.41	460–468	0	bsa	CCTKPESER
1120.73	[1;3]		1083.6		1121.55	161–168	1	bsa	YLYEIARR
1119.56; 1120.73; 1177.46	[7+8;5]; [1;3]; [7;5]; [8+9+10;3]	1120.6068	1138.6		1176.52	223–232	1	bsa	CASIQKFGER
1125.77; 1142.65	[1;3]; [8;4]	1124.7538	1142.71			548–557	1	bsa	KQTALVELLK
1158.55; 1177.46; 1200	[1;3]; [8+9+10;3]; [7+8;5]	1159.5986	1177.56	1199.54		300–309	0	bsa	ECCDKPLLEK
1248.7	[1;4]		1249.62			35–44	1	bsa	FKDLGEEHFK
1283.75	[1;3]; [2(+1);5]		1283.71	1305.69		361–371	0	bsa	HPEYAVSVLLR
1305.36	[2(+1);5]		1305.72			402–412	0	bsa	HLVDEPQNLIK
1290.65; 1289.77	[1;3]; [8;4]	1290.7665	1308.7			558–568	1	bsa	HKPKATEEQLK
1387.86	[4+5;3]		1349.5		1387.5	76–88	0	bsa	TCVADESHAGCEK
1387.86	[4+5;3]		1388.57			375–386	0	bsa	EYEATLEECCAK
1466.46	[8;4]; [8+9+10;3]		1429.5		1467.47	76–88	0	bsa	TCVADESHAGCEK PHOS: 82
1466.46; 1489.16	[8;4]; [4+5;3]; [8+9+10;3]		1466.59	1488.57		286–297	0	bsa	YICDNQDTISSK PHOS: 296
1535.96; 1536.05	[8;4]; [8+9+10;3]		1497.6		1535.59	387–399	0	bsa	DDPHACYSTVFDK
1557.9	[8+9+10;3]		1519.7		1557.7	139–151	0	bsa	LKPDPNTLCDEFK
1579.71	[8;4]; [8+9+10;3]		1578.6			267–280	0	bsa	ECCHGDLLECADDR
1640.21	[9+10;4]		1639.94			437–451	1	bsa	KVPQVSTPTLVEVSR

and BSA with a score 200 and 24 matches representing a sequence coverage of 37%. This approach unambiguously confirms the protein identification capabilities of LC-MS-SIMS. The resulting scores and sequence coverage demonstrate the potential of SIMS for peptide detection and protein identification through peptide mass fingerprinting.

3.4. *Imaging versus separation resolutions: perspectives for future developments*

The SIMS images provide the contour and distribution of LC fractions with high spatial resolution. SIMS imaging typically reaches sub-micron resolution, with modern atomic primary ion probes focused down to 50 nm. This spatial resolution can be taken further advantage of for the improvement of LC resolution. Our current LC deposition method where droplets are collected and spotted 1 mm apart every 30 s, limits the actual time separation (and LC time resolution) to time bins of 30 s. It is remarkable that with a similar deposition speed (1 mm in 30 s), the micron resolution of SIMS could correspond to a time resolution of 30 ms. This sampling rate available by LC-ME-SIMS is of the same order of magnitude than more common LC-MS couplings such as LC-ESI-FTICR. This demonstrates that MS imaging with SIMS is not limiting the separating power of LC. On the contrary it suggests that SIMS could more advantageously be coupled in future developments with higher efficiency and faster separation protocols, starting with shorter gradients more adapted to peptides separation.

In the current work however, the spatial resolution of the SIMS instrument is clearly out-performing the LC separation. This can be concluded from the observation that peptide traces usually span over several fractions in the image dataset, which means that peptides are eluted during rather broad time period. In our current conditions, each fraction corresponds to the accumulation of 30 s elution, therefore peptide presence in 2 fractions corresponds to an apparent elution time of about 1 min. Thus it can be concluded that in the current work, despite the relatively rough LC time resolution of the deposition technique used, the separation technique is the limiting factor. Nevertheless, we were able to separate, detect and assign a significant number of the expected digestion peptides for both Savinase and bovine serum albumin (see Tables 1 and 2). However, an optimized separation using for instance ultra performance liquid chromatography (UPLC) would decrease peptides overlap and concentrate peptide signal for increased S/N and detection efficiency.

The current work points out the possibilities of coupling high spatial resolution imaging techniques such as SIMS to

Table 3 – MASCOT search of the MSDB database for experimental [M+H] peaks from Tables 1 and 2 When unavailable, $[M+H]^+$ mass was reconstructed from observed adduct masses.

Bovalbumin nid: *Bos taurus* Match to: AAA51411 Score: **200** Expect: 3.2e-14 Nominal mass (M_r): 69248; Calculated pI value: 5.82 Number of mass values searched: 26 Number of mass values matched: 24 Sequence coverage: 37%	Synthetic mature subtilism 309 gene (fragment) Match to: CAA01797 Score: 128 Expect: 5.1e-07 Nominal mass (M_r): 26682; Calculated pI value: 9.30 Number of mass values searched: 12 Number of mass values matched: 10 Sequence coverage: 46%
1 MKWVTFISLL LLFSSAYSRG VFRRDTHK**SE IAHRFKDLGE EHFK**GLVLIA **51** FSQYLQQCPF DEHVKLVNEL TEFAK**TCVAD ESHAGCEK**SL HTLFGDELCK **101** VASLRETYGD MADCCEKQEP ERNECFLSHK DDSPDLPK**LK PDPNTLCDEF** **151** **K**ADEKKFWGK **YLYEIARR**HP YFYAPELLYY ANKYNGVFQE CCQAEDKGAC **201** LLPKIETMRE K**VLASSARQR** LR**CASIQKFG ER**ALKAWSVA RLSQKFPKAE **251** FVEVTKLVTD LTKVHK**ECCH GDLLECADDR** ADLAKYICDN QDTISSKLK**E** **301** **CCDKPLLEKS HCIAEVEK**DA IPENLPPLTA DFAEDKDVCK NYQEAKDAFL **351** GSFLYEYSRR **HPEYAVSVLL R**LAK**EYEATL EECCAKDDPH ACYSTVFDK**L **401** K**HLVDEPQNL IKQNCDQFEK** LGEYGFQNAL IVRYTR**KVPQ VSTPTLVEVS** **451** **R**SLGK**VGTRC CTKPESER**MP CTEDYLSLIL NRLCVLHEKT PVSEKVTK**CC** **501** **TESLVNR**RPC FSALTPDETY VPKAFDEKLF TFHADICTLP DTEKQIK**KQT** **551** **ALVELLKHKP KATEEQLK**TV MENFVAFVDK CCAADDKEAC FAVEGPK**LVV** **601** **STQTALA**	**1** **AQSVPWGISR VQAPAAHNRG LTGSGVKVAV LDTGISTHPD LNIR**GGASFV **51** PGEPSTQDGN GHGTHVAGTI AALNNSIGVL GVAPSAELYA VKVLGASGSG **101** SVSSIAQGLE WAGNNGMHVA NLSLGSPSPS ATLEQAVNSA TSR**GVLVVAA** **151** **SGNSGAGSIS YPAR**YANAM**A VGATDQNNNR** ASFSQYGAGL DIVAPGVNVQ **201** STYPGSTYAS LNGTSM**ATPH VAGAAALVKQ KNPSWSNVQI R**NHLK**NTATS** **251** **LGSTNLYGSG LVNAEAATR**
MASCOT search of MSDB database Peptide tolerance: 1.0 Da Trypsin Allowed 1 missed cleavage Sodiated C-terminus modification selected MH+ masses (from Table 2). Observed and reconstructed from adduct masses.	MASCOT search of MSDB database Peptide tolerance: 1.0 Da Trypsin/CNBr Allowed 1 missed cleavage Sodiated C-terminus modification selected MH+ masses (from Table 1). Observed and reconstructed from adduct masses.

separation techniques. To reach its full potential, it would benefit from coupling with micro-separation techniques of high separating power. Such a coupling would open doors to enhanced spectral decongestion and simplification, minimized ion suppression effects and in the end better sequence coverage, which leaves a large place for exciting perspectives for SIMS in the field of proteomics.

3.5. *Comparison with LC-MALDI and LC-ESI MS*

As shown previously, the sampling rate attainable by LC-ME-SIMS is not dissimilar to conventional LC-MS couplings. This is in part due to the fact that the separation by LC is decoupled from the actual MS measurement. Separation time is converted in separation position. In the present case, it is the resolving power of a TOF designed and optimized for low masses. However performing LC-ME-SIMS with another analyzer, e.g. an FT-ICR instrument, would add the benefits of high accuracy and resolving power.

The current measurements were performed with a tryptic digest of 20 nmol protein. This concentration initially seems high, but only 2 μL of the resulting digest was loaded on the column. Each LC sport on the ME-SIMS surface is estimated to contain significantly less that 100 pmol of peptides. As SIMS in the static mode samples less than 1% of the surface molecules this indicates that less than 1 pmol peptide is analyzed assuming all peptide molecules are on the matrix surface. Extended tests should be performed to evaluate the sensitivity of SIMS for high *m/z*, especially with C_{60} and high post acceleration voltages. ME-SIMS is currently implemented on a ToF instrument that is not optimized for proteomics. Additional sensitivity can be gained when dedicated instruments are constructed that take full advantage of modern mass spectrometers. Two aspects should be emphasized in the current ME-SIMS work. First, the observed signal intensity in absolute comparison with MALDI has to be paralleled with low sample consumption. The sensitivity *per* depth of sample removed already multiplies the observed sensitivity of SIMS (1–5 nm ablated) by a factor of 100 with regard to MALDI (often more than microns ablated). This point is further discussed in the following section. Secondly, the combination of matrix preparation with C_{60} primary ions and high post acceleration voltages results in peptide sensitivity in a mass range where SIMS had limited applicability for intact biomolecular analysis. As a result this work illustrates a major step forward for the technique.

3.6. *Unique advantage of SIMS: sample re-usability*

We have thus far shown that SIMS can be used in a normal proteomics workflow including peptide separation, mass measurement and database search for protein identification. Despite the sensitivity concerns expressed in the previous section, the results presented are thus far conclusive and encouraging. A non-negligible additional advantage of SIMS in this context is its low sample consumption. SIMS uses at most the top one to five nanometer layer of a sample, while in contrast with MALDI-MS up to microns of material are ablated off the surface at each laser shot. As a result of the low SIMS sample requirements, a sample such as our LC traces spotted on a matrix-coating is nearly untouched after the acquisition of one SIMS image and can be re-used for further analysis. Reproducibility of peptides signal could therefore be tested and peptide fingerprints could be confirmed for stable protein identification. Protein identification could be confirmed after a first imaging experiment by SIMS by careful parent ion selection and localization followed by MS/MS either by SIMS or MALDI on the same or the complementary tandem-MS mass spectrometer. Especially with SIMS tandem-MS, the choice of parent ions would not be limited in time such as for LC-ESI experiments, resulting from the decoupling of separation and mass measurement steps, or in sample abundance such as for

LC-MALDI experiments where sample is fully consumed during analysis. Sample analysis with LC-ME-SIMS would therefore be more flexible and complete. Given this multiple re-analysis capability, it would become meaningful and useful to store sample for later analysis and, in the longer term, create libraries of samples, similar to existing libraries of tissues embedded in paraffin that are stored in pathology departments of hospitals. Those libraries would be interesting to keep a trace of the history of an analysis and perform even later in time complementary analysis, looking for additional analytes, performing additional MS/MS analysis, etc.

4. Conclusions and perspectives

ME-SIMS in combination with C_{60}-primary ion gun enabled the identification by peptide mass fingerprinting of two large proteins digested with trypsin(–CNBr) after a LC-separation of the digested medium. This is the first time a coupling between SIMS and LC-separation has been shown, and demonstrates that SIMS is applicable for proteomics when combined with LC (for protein purification). The results of our study do not imply that LC-SIMS can immediately replace LC-MALDI, which is a very cost and time effective tool with well established protocols and routines and is gaining popularity. We would like to emphasize that the crippling limitations that once prohibited the use of SIMS in the proteomics field can be circumvented with the approach described in this paper. SIMS sensitivity, boosted by ME-SIMS and cluster/molecular primary ion beams, allows the detection without limitation of any digested peptide up to at least 5 kDa. Furthermore, using modern technology, SIMS profiling can be operated in comparable timescales to MALDI. Longer acquisition times can improve the applicability of LC-ME-SIMS as it will increase the overall analytical sensitivity.

The added value of SIMS is the re-usability of sample post analysis. This characteristic should be of considerable interest in studies where sample is scarce and where it is necessary to confirm the results with a second analysis. It is even possible to imagine building up libraries of sample available for additional/later analysis. Eventually, this characteristic should be particularly interesting when SIMS is used in combination with tandem-MS: in such case, the number of parents on which to perform MS/MS should not be limiting anymore, due to the very small sample consumption after each analysis.

Finally, coupling LC with ME-SIMS is of high interest for MSI applications. An important difficulty in imaging relates to the chemical complexity of tissue samples, giving rise to ion suppression effects: preferential ionization of certain compounds, formation of clusters, altogether reducing sensitivity and readability of the spectral information. To perform LC separation on adjacent tissue would remove those deleterious effects and provide a clearer view on the actual chemical composition of the tissue under investigation. Moreover, since mass analysis would be performed with the same ionization method, the LC-ME-SIMS experiments would provide a relevant database for direct analysis of tissue images acquired with ME-SIMS. Combined, the two approaches bring SIMS closer to proteomics standard methods and enable the identification and localization of proteins in biological surfaces at the cellular level.

Supplementary materials related to this article can be found online at doi:10.1016/j.jprot.2011.02.009.

Acknowledgements

This work is part of the research program of the “Stichting voor Fundamenteel Onderzoek der Materie (FOM)”, which is financially supported by the “Nederlandse organisatie voor Wetenschappelijk Onderzoek (NWO)”.

REFERENCES

[1] Vickerman JC, Briggs D. ToF-SIMS. Charlton, UK: IM Publications; 2001.
[2] McDonnell LA, Heeren RMA. Imaging mass spectrometry. Mass Spectrom Rev 2007;26:606–43.
[3] Chugtai K, Heeren RMA. Mass spectrometric imaging for biomedical tissue analysis. Chem Rev 2010;110:3237–77.
[4] John CM, Odom RW. Static Secondary Ion Mass Spectrometry (SSIMS) of biological compounds in tissue and tissue-like matrices. Int J Mass Spectrom Ion Processes 1997;161:47–67.
[5] Winograd N. Prospects for imaging TOF-SIMS: from fundamentals to biotechnology. Appl Surf Sci 2002;9192:1–7.
[6] Nygren H, Malmberg P, Kriegeskotte C, Arlinghaus HF. Bioimaging TOF-SIMS: localization of cholesterol in rat kidney sections. FEBS Lett 2004;566:291–3.
[7] Todd PJ, Schaaff TG, Chaurand P, Caprioli RM. Organic ion imaging of biological tissue with secondary ion mass spectrometry and matrix-assisted laser desorption/ionization. J Mass Spectrom 2001;36:355–69.
[8] Sjovall P, Lausmaa J, Johansson B. Mass spectrometric imaging of lipids in brain tissue. Anal Chem 2004;76:4271–8.
[9] Fartmann M, Kriegeskotte C, Dambach S, Wittig A, Sauerwein W, Arlinghaus HF. Quantitative imaging of atomic and molecular species in cancer cultures with TOF-SIMS and Laser-SNMS. Appl Surf Sci 2004;231–2:428–31.
[10] Altelaar AFM, Klinkert I, Jalink K, de Lange RPJ, Adan RAH, Heeren RMA, et al. Gold-enhanced biomolecular surface imaging of cells and tissue by SIMS and MALDI mass spectrometry. Anal Chem 2005;78:734–42.
[11] MacAleese LA, Stauber J, Heeren RMA. Perspectives for imaging mass spectrometry in the proteomics landscape. Proteomics 2009;9:819–34.
[12] Winograd N. The magic of cluster SIMS. Anal Chem 2005;77:142A–9A.
[13] Berman ESF, Wu LG, Fortson SL, Kulp KS, Nelson DO, Wu KJ. Chemometric and statistical analyses of ToF-SIMS spectra of increasingly complex biological samples. Surf Interface Anal 2009;41:97–104.
[14] McDonnell LA, Fletcher IW, De Lange RPJ, Heeren RMA. Higher sensitivity Secondary Ion Mass Spectrometry of biological molecules for high resolution, chemically specific imaging. J Am Soc Mass Spectrom 2006;17:1195–202.
[15] Wagner MS, Castner DG. Analysis of adsorbed proteins by static time-of-flight secondary ion mass spectrometry. Appl Surf Sci 2004;231:366–76.
[16] S. Sole-Domenech, B. Johansson, M. Schalling, J. Malm, P. Sjovall. Analysis of opioid and amyloid peptides using Time-of-Flight Secondary Ion Mass Spectrometry. Anal Chem 2010;82:1964–74.
[17] Eijkel GB, Kukrer-Kaletas B, van der Wiel IM, Kros JM, Luider TM, Heeren RMA. Correlating MALDI and SIMS imaging mass spectrometric datasets of biological tissue surfaces. Surf Interface Anal 2009;41:675–85.